

Yield statistics of interpolated superoscillations

Eytan Katzav

Racah Institute of Physics, the Hebrew University, Jerusalem 91904, Israel

Ehud Perlsman and Moshe Schwartz

Department of Physics, Raymond and Beverly Sackler Faculty Exact
Sciences, Tel Aviv University, Tel Aviv 69978, Israel

Abstract - Yield Optimized Interpolated Superoscillations (YOIS) have been recently introduced as a means for possibly making the use of the phenomenon of superoscillation practical. In this paper we study how good is a superoscillation that is not optimal. Namely, by how much is the yield decreased when the signal departs from the optimal one. We consider two situations. One is the case where the signal strictly obeys the interpolation requirement and the other is when that requirement is relaxed. In the latter case the yield can be increased at the expense of deterioration of signal quality. An important conclusion is that optimizing superoscillations may be challenging in terms of the precision needed, however, storing and using them is not at that sensitive. This is of great importance in physical systems where noise and error are inevitable.

Superoscillatory signals are band limited functions that oscillate over some regions with a frequency larger than that of its maximal Fourier component. A number of examples have been given in the past for such functions with very interesting applications in quantum mechanics [1]-[6], signal processing [7]-[13] and in optics, where super oscillations are intimately related to super

resolution [14]-[16] with some recent exciting experimental achievements [17]-[18]. For a recent review see [19].

A key issue in the field is quantifying the superoscillations using some local frequency, e.g. the local rate of change of the phase of the signal among others [20]. Another question of much interest is how superoscillations interact with physical matter during propagation [21]-[22], with some indication (both theoretically [23] and experimentally [24]) that nonlinearities may actually become play an important role in utilizing them.

However, although the phenomenon of superoscillation suggests many practical applications, its uses are presently rather limited, because the superoscillatory signal exist in limited intervals and that the amplitude of the superoscillation in those regions is extremely small compared to typical values of the amplitude in non-superoscillating regions [2], [10], [11]. This often renders algorithms for generating them generically numerically unstable [25]. One of the methods for obtaining superoscillations that lends itself easily to improving the situation described above, is that of forcing interpolation within the prescribed interval, that will necessarily, lead to the required superoscillation [26].

We start our discussion by explaining the concept of interpolated superoscillation [11, 26]. Consider the signal

$$f(t) = \frac{A_0}{\sqrt{2\pi}} + \sum_{m=1}^N \frac{A_m}{\sqrt{\pi}} \cos(mt) , \quad (1)$$

which is periodic in $t \in [-\pi, \pi]$. Choose a sub-interval $[0, a]$ with $a < \pi$ and impose on the function $f(t)$ M constraints in the interval, such that $f(t_j) = \mu_j$

for $0 \leq t_j \leq a$ and $j=0, \dots, M-1$. The constraints result in a set of M linear equations in $N+1$ unknowns of the form,

$$\sum_{m=0}^N C_{jm} A_m \equiv \mathbf{C}_j \cdot \mathbf{A} = \mu_j, \quad (2)$$

where $C_{jm} = \frac{1}{\sqrt{\pi}} \begin{cases} \cos(mt_j) & \text{for } m \neq 0 \\ 1/\sqrt{2} & \text{for } m = 0 \end{cases}$.

Generically this set of equations: has no solution for $M > N+1$, has one solution for $M = N+1$ and a whole space of solutions for $M < N+1$. A particular choice of great interest [26] is

$$t_j = \frac{a}{(M-1)} j \quad \text{and} \quad \mu_j = (-1)^j \quad j=0, \dots, M-1. \quad (3)$$

Provided $M \leq N+1$, this choice constrains the function to oscillate within the interval $[-a, a]$ between the values ± 1 with a frequency

$$\omega = \frac{\pi(M-1)}{a}. \quad (4)$$

It is thus clear that the frequency of oscillation within the interval $[-a, a]$ can be increased indefinitely regardless of the largest harmony $\cos(Nt)$ included in the signal (1). As is well known, this comes, at a cost. The amplitude in the superoscillatory region is extremely small relative to the total energy. Therefore optimization is required if the use of the phenomenon of superoscillation is to become practical.

Next we, would like to optimize our superoscillating function for fixed a and $M < N+1$ but we have to decide first in what sense we want to optimize it. One approach in the literature [11, 27] is to consider the energy of the signal,

$$E = \int_{-\infty}^{\infty} f^2(t) dt, \quad \text{use the fact that } f \text{ is band limited and minimize the energy}$$

under the interpolation constraints. In the periodic function case, the

equivalent would be to minimize, $E = \int_{-\pi}^{\pi} f^2(t)dt$ under the choice of the Fourier coefficients given by equation (1). A step forward would be to maximize the superoscillation yield,

$$Y(M, a) = \frac{\int_{-a}^a f^2(t)dt}{\int_{-\pi}^{\pi} f^2(t)dt}, \quad (5)$$

rather than the total energy. As will become evident in the following the two methods of optimization are very close to each other, provided the optimal yield is indeed very small, which in many situations is the case. It is easy to show that the yield is given by,

$$Y(N, M, a) = \frac{\int_{-a}^a f^2(t)dt}{\int_{-\pi}^{\pi} f^2(t)dt} = \frac{\sum_{m,n=0}^N \Delta_{mn} A_m A_n}{\sum_{m=0}^N A_m^2} \equiv \frac{I}{D}, \quad (6)$$

where the entries of the matrix Δ are given by

$$\Delta_{mn} \equiv \begin{cases} \frac{2}{\pi} \frac{[m \cos(ma) \sin(na) - n \cos(na) \sin(ma)]}{m^2 - n^2} & \text{for } m \neq n \neq 0 \\ \frac{1}{\pi} \left[a + \frac{\sin(2na)}{2n} \right] & \text{for } m = n \neq 0 \\ \frac{\sqrt{2}}{n} \sin(na) & \text{for } m = 0 \text{ and } n \neq 0 \\ \frac{a}{\pi} & \text{for } m, n = 0 \end{cases} \quad (7)$$

To affect the optimization of the yield [26], the original degrees of freedom, are rotated in such a way, going from the original set of the A's to a new set of degrees of freedom B, as to break the linear N+1 dimensional space, into a direct sum of two subspaces. The first M dimensional subspace is the space, S_M , where the M independent B's are independently constrained and attain prescribed values determined by the constraints. Thus, from all that

subspace, we choose a specific vector \mathbf{B}_M^C . The remaining $(N+1-M)$ -dimensional subspace, \mathcal{S}_{N+1-M} , is totally unconstrained.

The set of interpolating signals is defined thus by

$$\mathbf{B} = \mathbf{B}_{N+1-M} + \mathbf{B}_M^C \quad (8)$$

where $\mathbf{B}_{N+1-M} \in \mathcal{S}_{N+1-M}$.

In ref. [26] we have optimized the yield under the interpolation constraints. In the following we address the question of the distribution of the yield in the subspace of interpolating signals. This is relevant to the question - by how much is a typical superoscillation worse than the optimal.

Consider next the functional dependence of the yield on the constrained and on the unconstrained B 's. The numerator I on the right hand side of equation (6), can be expressed as follows

$$I = \sum_{m,n=0}^N \Delta_{mn} A_m A_n = \sum_{m,n=0}^N \Delta^{(R)}_{mn} B_m B_n \quad (9)$$

where $\Delta^{(R)} = \mathbf{R}\Delta\mathbf{R}^{-1}$, \mathbf{R} being the rotation that takes the coefficient vector \mathbf{A} into \mathbf{B} . Let us describe the matrix $\Delta^{(R)}$ by the following block form

$$\Delta^{(R)} = \begin{pmatrix} \tilde{\Delta}_{(N+1-M) \times (N+1-M)} & \Gamma_{(N+1-M) \times M} \\ \Gamma^T_{M \times (N+1-M)} & \bar{\Delta}_{M \times M} \end{pmatrix} \quad (10)$$

where Γ^T is the transpose of Γ . The yield can now readily be expressed in terms of the unconstrained B 's is

$$Y = \frac{I}{D} = \frac{\sum_{m,n=0}^{N-M} \tilde{\Delta}_{mn} B_m B_n + 2 \sum_{m=0}^{N-M} \sum_{n=N+1-M}^N \Gamma_{mn} B_n^C B_m + \sum_{m,n=N+1-M}^N \bar{\Delta}_{mn} B_m^C B_n^C}{\sum_{m=0}^{N-M} B_m^2 + \sum_{m=N+1-M}^N (B_m^C)^2} \quad (11)$$

To simplify the notation we rewrite

$$Y = \frac{\sum_{mn=0}^{N-M} \tilde{\Delta}_{mn} B_m B_n + \sum_{m=0}^{N-M} \alpha_m B_m + D_1}{\sum_{m=0}^{N-M} B_m^2 + D_2}, \quad (12)$$

where the symmetric positive definite matrix $\tilde{\Delta}$, the coefficients α_m and the constants D_1 and D_2 depend on the interpolation constraints (and also on the specific frame of reference used in the S_M subspace). We would like to take a random set of B 's and get an idea of the corresponding random yield as a consequence. A random choice of the B 's would typically mean very large B 's. This means that for such a choice the yield would be typically given by

$$Y \approx \frac{\sum_{m,n=0}^{N-M} \tilde{\Delta}_{mn} B_m B_n}{\sum_{m=0}^{N-M} B_m^2} \quad (13)$$

Thus, it is clear that typically, the value of Y is distributed between the largest and smallest eigenvalue of $\tilde{\Delta}$, which spans many decades (the condition number of $\tilde{\Delta}$ is very large). To give just two examples, the largest and smallest eigenvalues of $\tilde{\Delta}$ ($\delta_{\max}, \delta_{\min}$) for the cases of $N=6, M=4$ and $N=9, M=6$ are given by $(0.000179, 3.12 \cdot 10^{-14})$ and $(4.65 \cdot 10^{-6}, 3.64 \cdot 10^{-21})$ respectively. It is interesting to note that the corresponding optimal values of the yield are $Y=0.0138$ (for $N=6, M=4$) and $Y=0.0004$ (for $N=9, M=6$). This implies that a random choice of a signal that interpolates the constrained points gives a yield which is **orders of magnitude** less than the optimal one, which again emphasizes the necessity in optimizing the signals.

At this point we can say more about the statistical properties of the yield of interpolating signals. We will assume first that the B 's are uncorrelated and have an identical distribution

$$P(B) = \frac{1}{\sigma} g\left(\frac{B}{\sigma}\right), \quad (14)$$

where $g(x)$ is a normalized and symmetric distribution. We will consider averages as a function of σ and then distributions for fixed σ . We start with some obvious results: it is clear that

$$\lim_{\sigma \rightarrow 0} Y = \frac{D_1}{D_2}. \quad (15)$$

This gives, combined with equation (13), a lower bound on the optimal yield, namely

$$Y_{opt} > \max\left(\frac{D_1}{D_2}, \delta_{\max}\right). \quad (16)$$

Consider next the very simple average of the total energy per period (the denominator of Y – eq. (5))

$$\langle E \rangle = (N + 1 - M)\sigma^2 + D_2, \quad (17)$$

which turns out to be independent of the specific distribution. The average yield is however more difficult and does depend on the distribution. Let us therefore discuss a few illustrative examples. Consider first the bimodal

distribution, $P(B) = \frac{1}{2\sigma} \left[\delta\left(\frac{B}{\sigma} - 1\right) + \delta\left(\frac{B}{\sigma} + 1\right) \right]$, where δ is the Dirac

delta function. The average yield in this case is simple

$$\langle Y \rangle = \frac{(tr\tilde{\Delta})\sigma^2 + D_1}{(N + 1 - M)\sigma^2 + D_2}. \quad (18)$$

Consider next a Gaussian distribution, $P(B) = \frac{1}{\sqrt{2\pi}\sigma} \exp\left(-\frac{B^2}{2\sigma}\right)$.

Although considerably more complicated, the average yield can also be obtained analytically here,

$$\langle Y \rangle = \frac{D_1}{2\sigma^2} e^{\frac{D_2}{2\sigma^2}} E_{\frac{N+1-M}{2}}\left(\frac{D_2}{2\sigma^2}\right) + \frac{tr\tilde{\Delta}}{2} e^{\frac{D_2}{2\sigma^2}} E_{\frac{N+3-M}{2}}\left(\frac{D_2}{2\sigma^2}\right) \quad (19)$$

where $E_\nu(z) = \int_1^\infty dx \frac{\exp(-xz)}{x^\nu}$, is the exponential integral function [18]. It is

clear from equations (13) and (15) that regardless of the distribution the

average has to interpolate between $\frac{D_1}{D_2}$ at small σ and $\frac{tr\tilde{\Delta}}{N + 1 - M}$,

is the average eigenvalue of $\tilde{\Delta}$ at large σ . The two averages, (18) and (19) are presented in Figs. 1 and 2 for the cases $N = 6, M = 4$ and $N = 9, M = 6$, respectively.

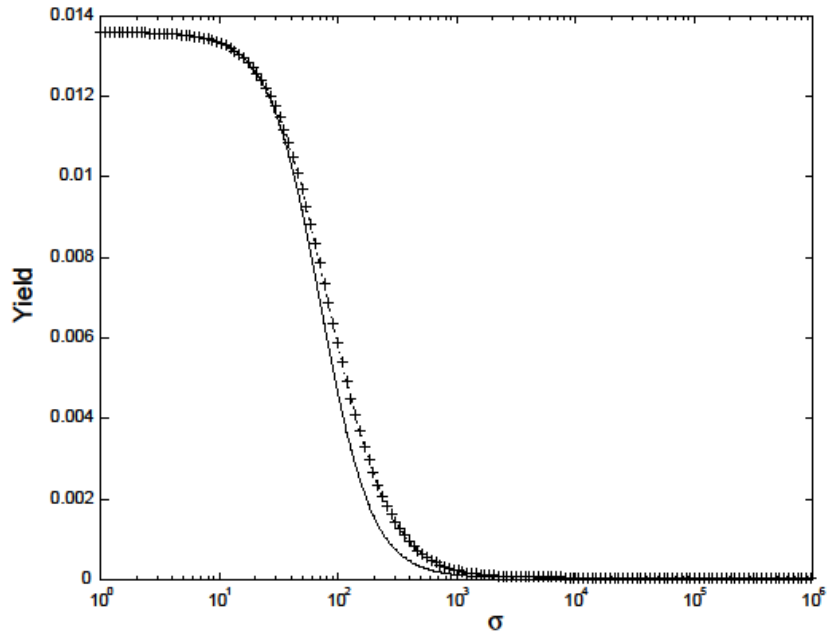


Fig. 1 The average yield $\langle Y \rangle$ as a function of the σ for $N=6, M=4$. The upper curve is for the Gaussian distribution (given by eq. (19)) and the lower one for the bimodal distribution (given by eq. (18)).

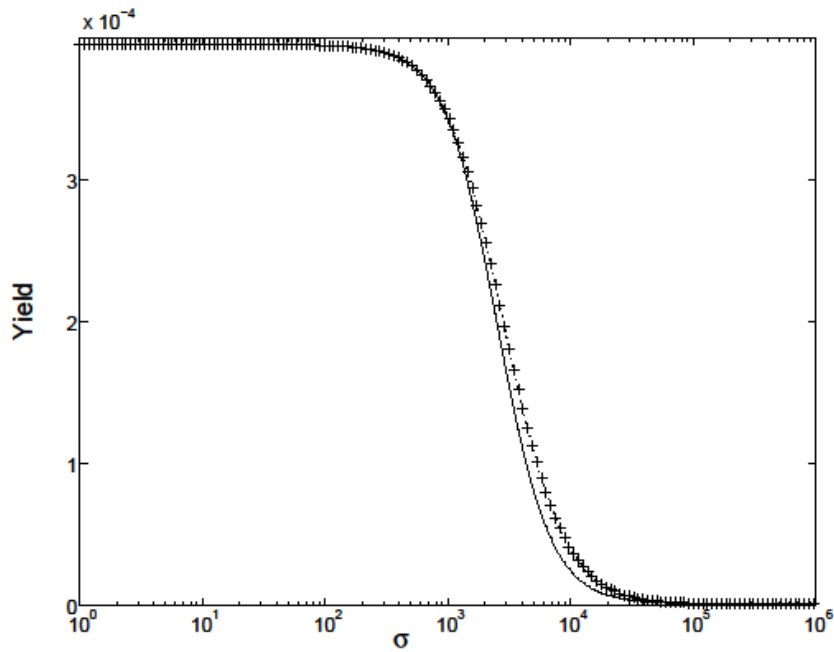


Fig. 2 The average yield $\langle Y \rangle$ as a function of the σ for $N=9, M=6$. The upper curve is for the Gaussian distribution (given by eq. (19)) and the lower one for the bimodal distribution (given by eq. (18)).

It is clear from the above figures that although $\langle Y \rangle$ depends on the precise distribution of the B's, this dependence is not very pronounced. Both cases result in $\langle Y \rangle$ which behaves like a sigmoid, namely it stays very close to $\langle Y \rangle(\sigma=0)$ until it drops to zero over a relatively short range. This is indicative of the presence of a phase transition or a sharp crossover as a function of the noise level.

The two figures above are not conclusive concerning whether for large σ the ratio of the average yield obtained from the Gaussian distribution to that obtained from the bimodal distribution tends to one, as predicted above (Figs. 1 and 2 only show that both tend to zero). Therefore, we present the ratio of the two for the case $N=6, M=4$ in Fig. 3 (the same figure for the case $N=9, M=6$ is quite similar and will not be presented here for brevity).

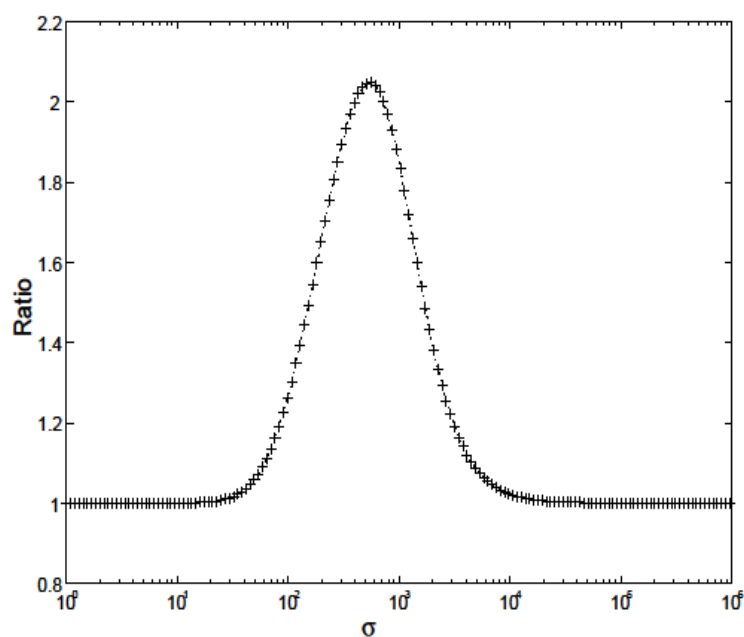


Fig. 3 The ratio between the average yield for the Gaussian distribution (given by eq. (19)) and that for the bimodal distribution (given by eq. (18)) as a function of σ for $N=6, M=4$.

It is of interest to obtain also the second moment of the yield. This calculation can also be performed analytically even for the Gaussian distribution but we will not present it in the following, because it is considerably more complicated and lengthy. In the Figs. 4 - 5 we present the ratio of second to first moment (namely, $\langle Y^2 \rangle / \langle Y \rangle^2$) for the case $N=6, M=4$ and the two distributions.

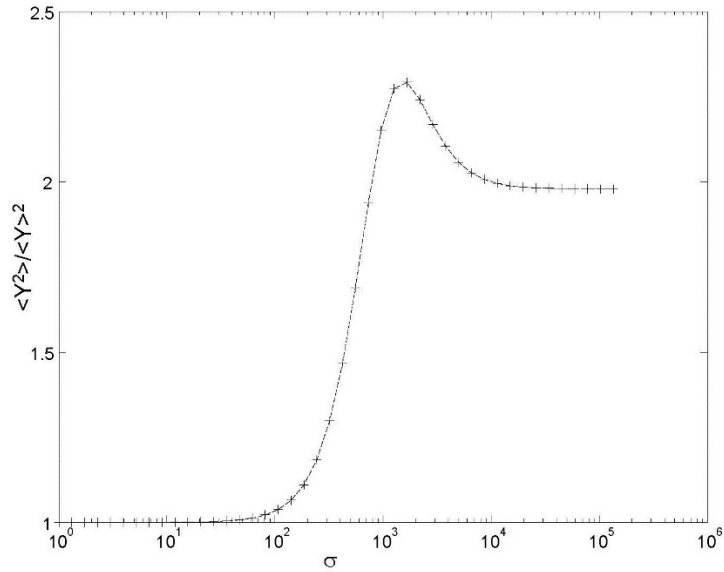


Fig. 4 The ratio between the second moment of the yield and the square of the mean $\langle Y^2 \rangle / \langle Y \rangle^2$ for the bimodal distribution as a function of σ for $N = 6, M = 4$.

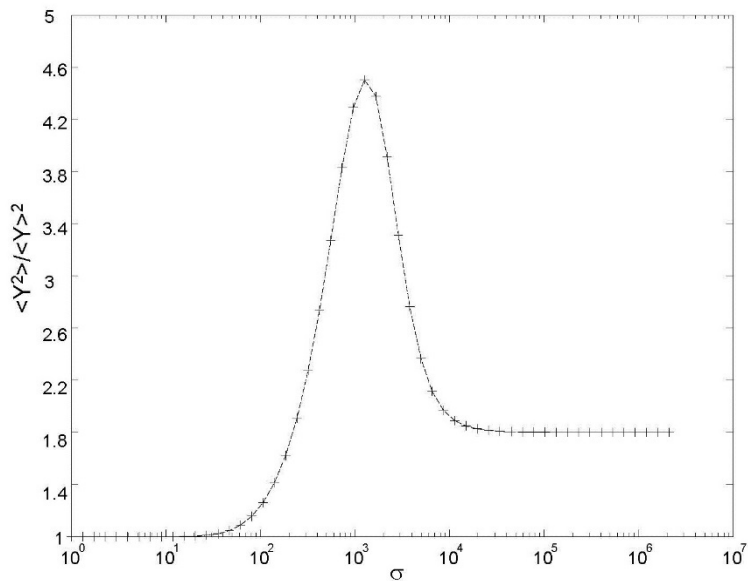


Fig. 5 The ratio between the second moment of the yield and the square of the mean $\langle Y^2 \rangle / \langle Y \rangle^2$ for the Gaussian distribution as a function of σ for $N = 6, M = 4$.

Considering figures 4 - 5 it becomes clear that the yield distribution behaves differently for three distinct regions of σ . Indeed, that is the case as presented in Fig. 6 depicting yield distributions for three representative values of σ .

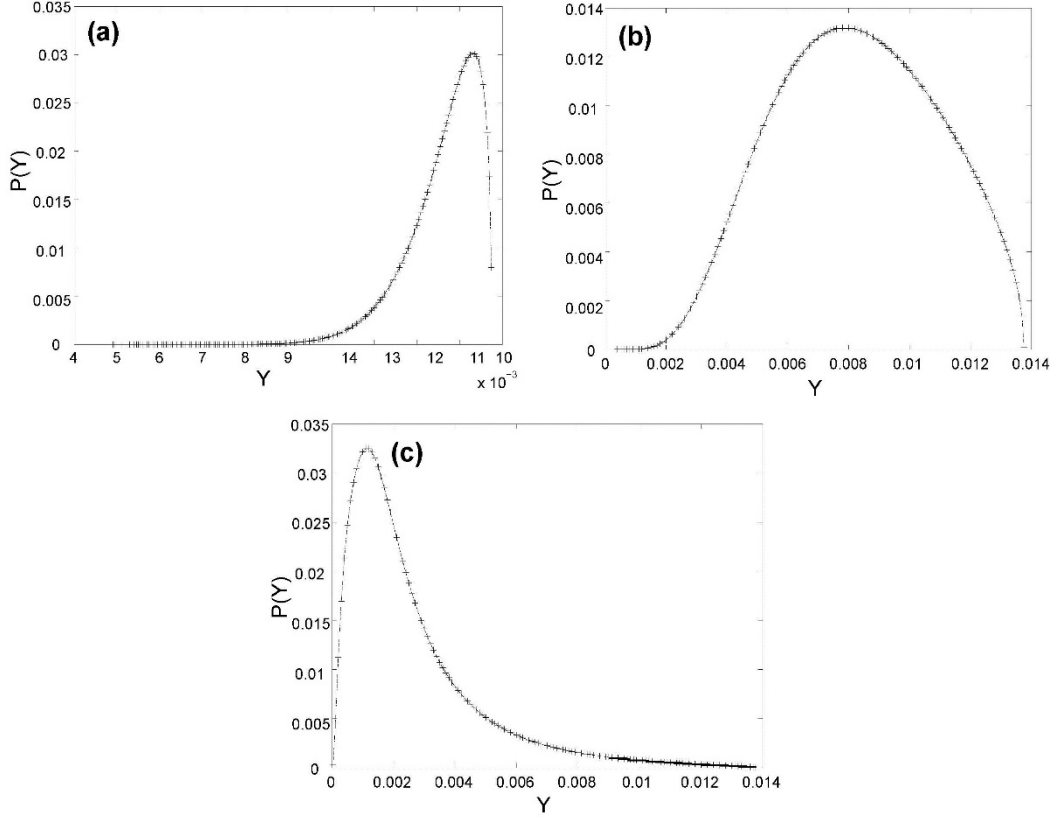


Fig. 6 The distribution of the Yield for three different representative values of σ for $N=6, M=4$: (a) $\sigma=20$, (b) $\sigma=65$ and (c) $\sigma=200$, corresponding to the three regions identified in Fig. 3.2. As can be seen, the distributions are indeed very different with pronounced skewness in opposite directions.

It follows from the above figures that the average yield and its standard deviation are monotonically decreasing functions of σ . Does it mean that the optimal yield is characterized by very small B 's? To answer this considers the total energy (per period).

$$E = D = \sum_{m=0}^{N-M} B_m^2 + D_2 . \quad (20)$$

It is clear that the total energy is minimized when $B_m = 0$ for $0 \leq m \leq N-M$ and the minimal total energy per period is D_2 . We note further that the total energy can be expressed as $E = \frac{I}{Y}$. Thus the (very simple) minimization process of E with respect to the choice of the B_m 's, can be expressed as

$$\frac{1}{Y} \frac{\partial I}{\partial B_m} - \frac{I}{Y^2} \frac{\partial Y}{\partial B_m} = 0 . \quad (21)$$

Consequently, on the set of B 's for which the total energy per period is minimized we have

$$\frac{\partial Y}{\partial B_m} = Y \frac{\partial I}{\partial B_m} , \quad (22)$$

and since Y is typically very small (in the superoscillatory regime), we conclude that at the point of minimal total energy, the yield is almost extremal (i.e., maximal) too, because the absolute value of each of its derivatives is very small. Conversely, the B 's at the optimal yield are very small, as expected from the σ dependence of the average yield. Thus, optimization of the total energy under the constraints (at least in the superoscillatory regime) is generically almost equivalent to optimization of the yield itself.

So far, we have considered the behavior of the yield in the space of interpolating signals, i.e. in the subspace where the B 's automatically obey the constraints. Next we address the question of possible departure of the signal from the prescribed interpolation, in the vicinity of the yield optimized interpolating signal. Such departure will no doubt happen in any physical device that would need to utilize such signals, because any realization of a superoscillatory signal using a Fourier representation (1) would have access to the set of A 's with finite precision (due to the presence of noise for example). Such limited precision will obviously affect the yield, but of not less importance, it could also imply violation of the interpolation constraint, which may eventually destroy the superoscillatory nature of the signal. Recall that the yield is maximized with respect to the choice of the A_m 's under the constraints given by equations (2)-(3). The result is a set of optimal Fourier coefficients $\{\tilde{A}_m\}$. To address the questions of violation of the constraints due to finite precision, assume that the actual Fourier coefficients describing the superoscillating function are given by

$$\hat{A}_m = \tilde{A}_m + \delta_m , \quad (23)$$

where δ_m 's are random errors and governed by a Gaussian distribution with standard deviation δ . Consider the first question, which is the sensitivity of the interpolation to random fluctuations around the optimal solution. Equations (2)-(3) imply that the change in the value of the function $f(t)$ at the points $t_j = ja/(M-1)$ for $j=0, \dots, M-1$, is given by

$$\delta f_j = \sum_{m=1}^N C_{jm} \delta_m , \quad (24)$$

where all the absolute values of all the C_{jm} 's are less or equal to 1 (by definition – see eq. (2)). Consequently,

$$|\delta f_j| \propto \delta \sqrt{N} . \quad (25)$$

Now, as long as the right hand side is (considerably) less than one we still have

$$\text{sign}[f(t_j)] = (-1)^j , \quad (26)$$

so that the number of oscillations in the interval $[0, a]$ does not decrease and thus the required superoscillation is still preserved.

To what extent do the fluctuations around the yield-optimized signal affect the required superoscillation? Put differently, what is the error level δ that would start impairing the required superoscillations? Form eqs. (25)-(26) it is clear that the required absolute accuracy is

$$\delta < 1/\sqrt{N} , \quad (27)$$

which does not seem to pose a serious problem.

Note, however, that the problem might be that the error δ can be reduced only below a value which is relative to the typical absolute value of the A 's. If that is the case it might pose a severe problem, because the optimal Fourier amplitudes are exponentially large in N (for superoscillating signals) and this is why out of the superoscillating interval the absolute value of f is exponentially large in N . In that case, the relative accuracy required in the Fourier coefficients is of the order of $\theta = \delta/|A| \propto N^{-1/2} \alpha^{-N}$, where $|A|$ denotes the typical size of the \tilde{A}_m 's and $\alpha > 1$. Thus, if it is only relative accuracy that is possible to control, care should be taken that N is not too large in order to preserve the superoscillations. If absolute accuracy can be obtained, regardless of the magnitude of the optimal Fourier coefficients, it should be no problem to preserve superoscillations under very considerable fluctuations in those quantities. We characterize the departure from the enforced interpolation, for a given set of errors in the Fourier coefficients by a single parameter,

$$\delta V = \frac{1}{M} \sum_{i=0}^{M-1} (\delta f_i)^2 . \quad (28)$$

Figures 7 - 8 give the interpolation sensitivity, which is the average of δV over the Gaussian distribution of the δ_m 's, as a function of δ for two examples of yield optimized superoscillations,

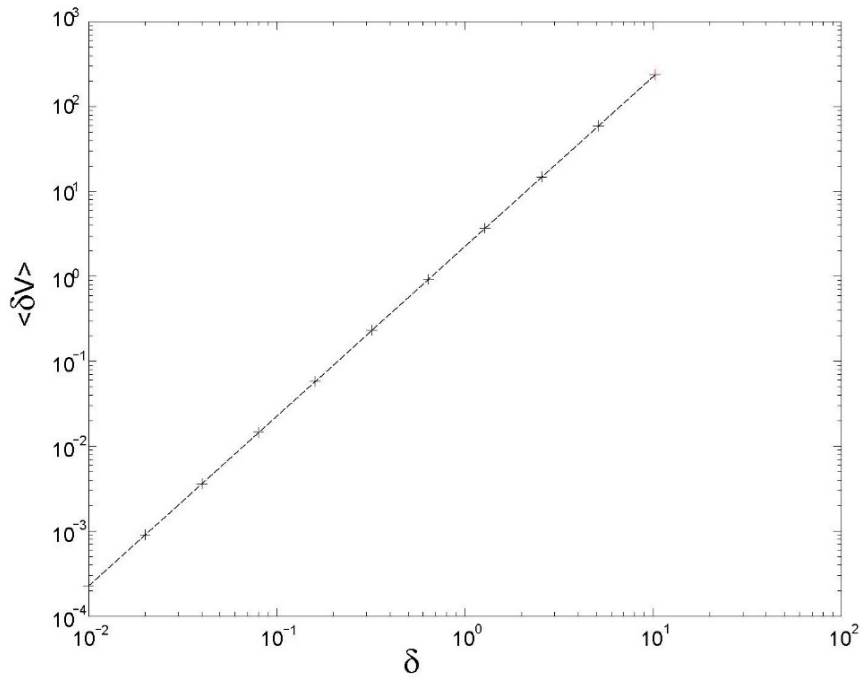


Fig. 7 - The mean interpolation sensitivity $\langle \delta V \rangle$ as a function of δ for $N = 6, M = 4$.

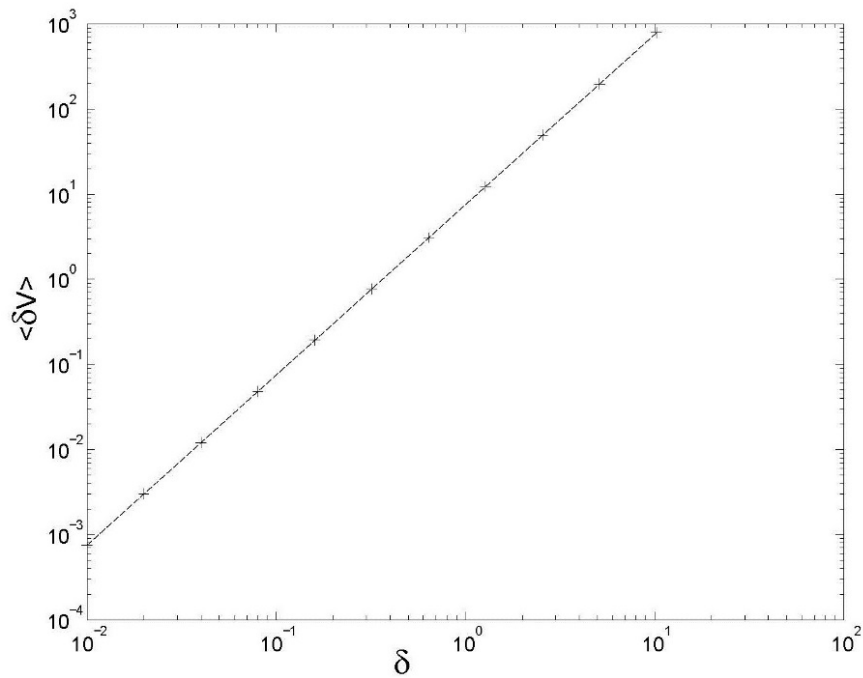


Fig. 8- The mean interpolation sensitivity $\langle \delta V \rangle$ as a function of δ for $N = 12, M = 8$

Note that in spite of the fact that in the graphs the δ attain values up to 10^2 , only for δ 's considerably smaller than one, we may expect the original frequency in the superoscillating interval to be unchanged. (The oscillation period, T , is taken as the average peak to peak distance and the frequency is $\omega = 2\pi/T$.)

While the interpolation sensitivity $\langle \delta V \rangle$ is an important quantity that characterizes the deviations from the enforced interpolation, it is, obviously, not less important to obtain the distribution of the quantity δV . In the following we give this distribution for the case $N = 12$, $M = 8$ and for a specific value of $\delta = 0.01$. It is clear that at least as far as the order of magnitude is considered, the interpolation sensitivity represents well the distribution of the values of δV . The distribution is obtained by considering 10^7 realizations of the set of the low frequency Fourier coefficients.

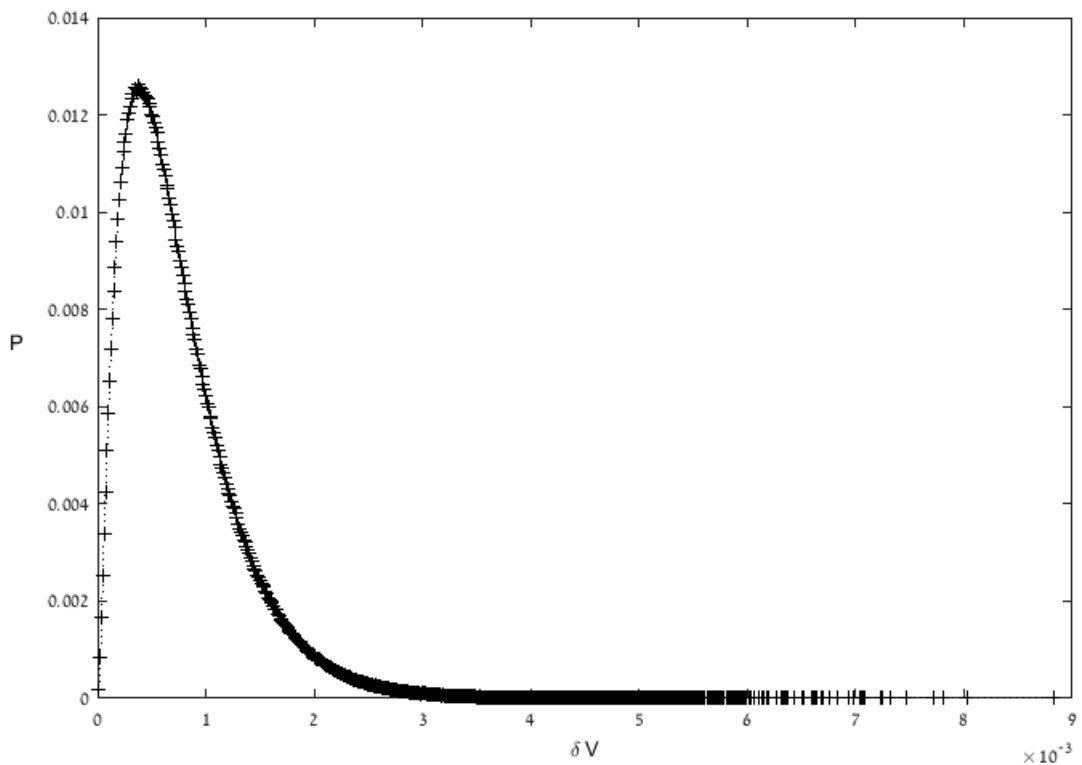


Fig. 9 –The normalized distribution, $P(\delta V)$, for $\delta = 0.01$. The distribution is obtained from 10^7 realizations of the set of Fourier coefficients.

The next problem is that of the sensitivity of the superoscillation yield. The yield can be expressed in terms of the deviations as follows. The deviations from the optimal Fourier coefficients define a function giving the deviation from the optimal function, $\tilde{f}(t)$, obeying the constraints, namely

$$\delta(t) = \frac{\delta_0}{\sqrt{2\pi}} + \sum_{m=1}^N \frac{\delta_m}{\sqrt{\pi}} \cos(mt) . \quad (29)$$

The first order change in the yield can be written in terms of this function as

$$\delta Y = 2 \frac{\int_{-\pi}^{\pi} \tilde{f}(t) \delta(t) dt}{\int_{-\pi}^{\pi} \tilde{f}^2(t) dt} - 2Y \frac{\int_{-\pi}^{\pi} \tilde{f}(t) \delta(t) dt}{\int_{-\pi}^{\pi} \tilde{f}^2(t) dt} . \quad (30)$$

The fact that the yield has a linear correction when calculated at its maximum, should not be surprising, because it is a constrained maximum and the linear part appears as a result of the small violations of the strict interpolation constraint. Had we considered deviations in the Fourier coefficients that respect the constraints, the lowest order correction would be quadratic in $\delta(t)$. This implies that because of the departure from the interpolation constraints, the yield can increase under fluctuations. In the Figs. 10 and 11 we give the average of δY , as a function of δ . As we shall see, the average, which is not the average of the linear approximation of δY given above, is positive. This will be explained later when the scatter graph, giving the distribution of pairs $(\delta V, \delta Y)$ for given δ will be discussed.

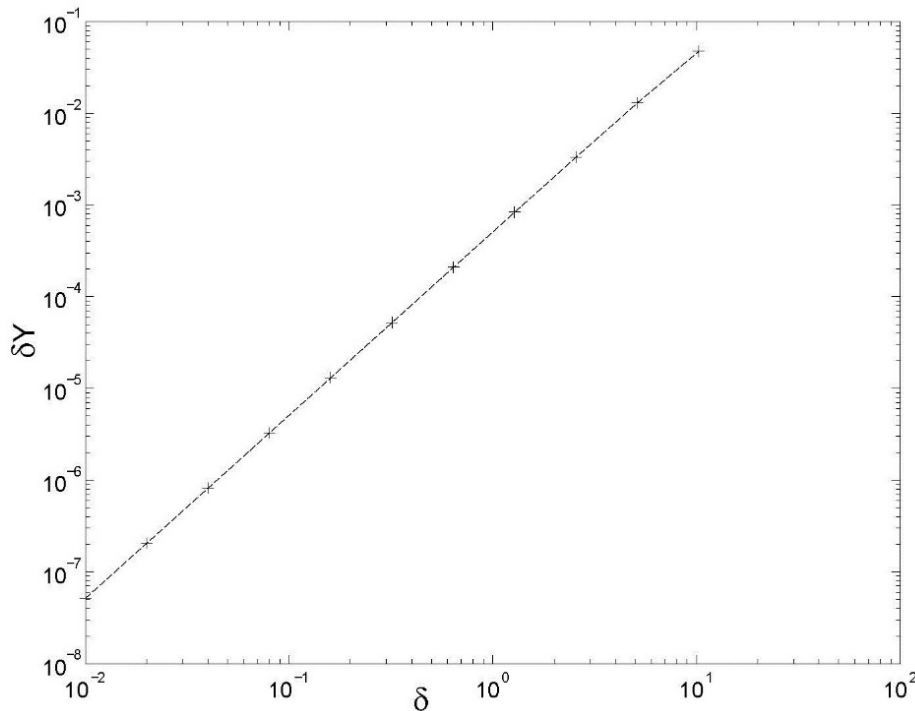


Fig. 10- The average deviation of the yield as a function of δ for $N = 6, M = 4$

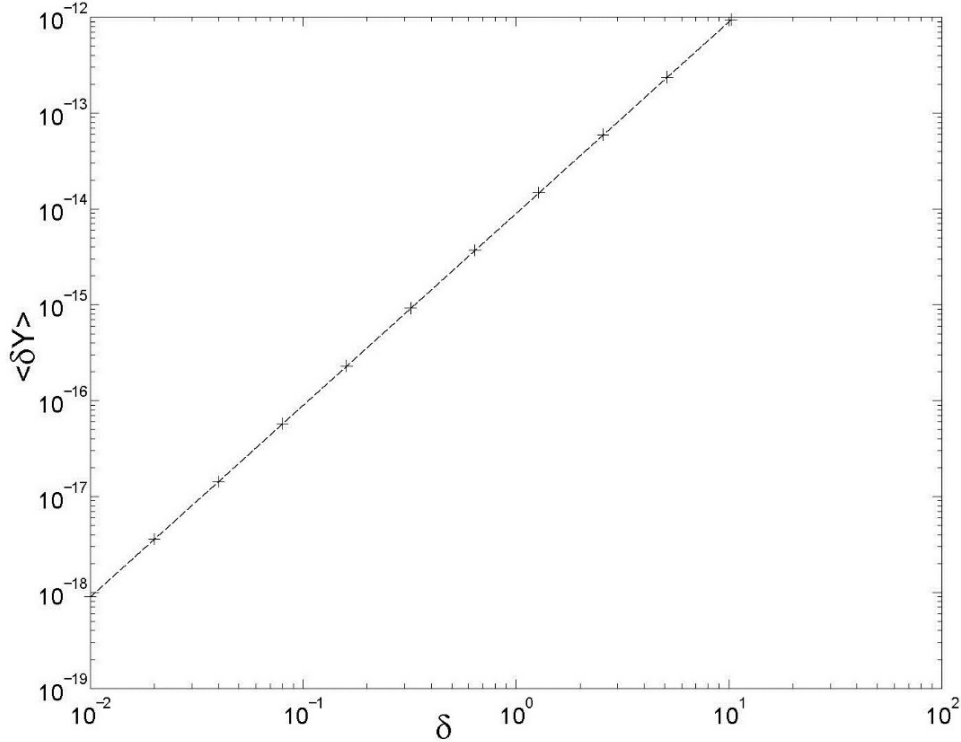


Fig.11- The average deviation of the yield as a function of δ for $N = 12, M = 8$

The relative deviation in the yield is given by

$$\frac{\delta Y}{Y} = \frac{\int_{-a}^a \tilde{f}(t) \delta(t) dt}{\int_{-a}^a \tilde{f}^2(t) dt} - 2 \frac{\int_{-\pi}^{\pi} \tilde{f}(t) \delta(t) dt}{\int_{-\pi}^{\pi} \tilde{f}^2(t) dt} . \quad (31)$$

An upper bound on the relative error in the yield can be obtained now by noting first that a t -independent bound on the mean square deviation function is easily obtained from equation (29),

$$\langle \delta^2(t) \rangle < \frac{N}{\pi^2} \delta^2 . \quad (32)$$

Then the error in the yield clearly obeys

$$\frac{|\delta Y|}{Y} < 2 \left[\frac{\left| \int_{-a}^a \tilde{f}(t) \delta(t) dt \right|}{\int_{-a}^a \tilde{f}^2(t) dt} + \frac{\left| \int_{-\pi}^{\pi} \tilde{f}(t) \delta(t) dt \right|}{\int_{-\pi}^{\pi} \tilde{f}^2(t) dt} \right] \quad (33)$$

and by the Schwartz inequality and equation (12) above,

$$\frac{|\delta Y|}{Y} < \frac{4\sqrt{N}\delta}{\pi} \left[\sqrt{\frac{a}{\int_{-a}^a \tilde{f}^2(t) dt}} + \sqrt{\frac{\pi}{\int_{-\pi}^{\pi} \tilde{f}^2(t) dt}} \right]. \quad (34)$$

The second term in the square brackets above can be neglected compared to the first and taking into account that within the superoscillating interval, $\tilde{f}^2(t)$ is of order 1, we arrive at the conclusion that

$$\frac{|\delta Y|}{Y} < \beta \sqrt{\frac{N}{a}} \delta. \quad (35)$$

where β is a constant of order 1.

Thus, if the condition for the preservation of superoscillation in the presence of additive errors in the optimal Fourier coefficients $\{\tilde{A}_m\}$ is obeyed, it ensures automatically an upper bound on the error in the yield. In Figs. 12 - 13 we show the average relative error in the yield, which we call yield sensitivity.

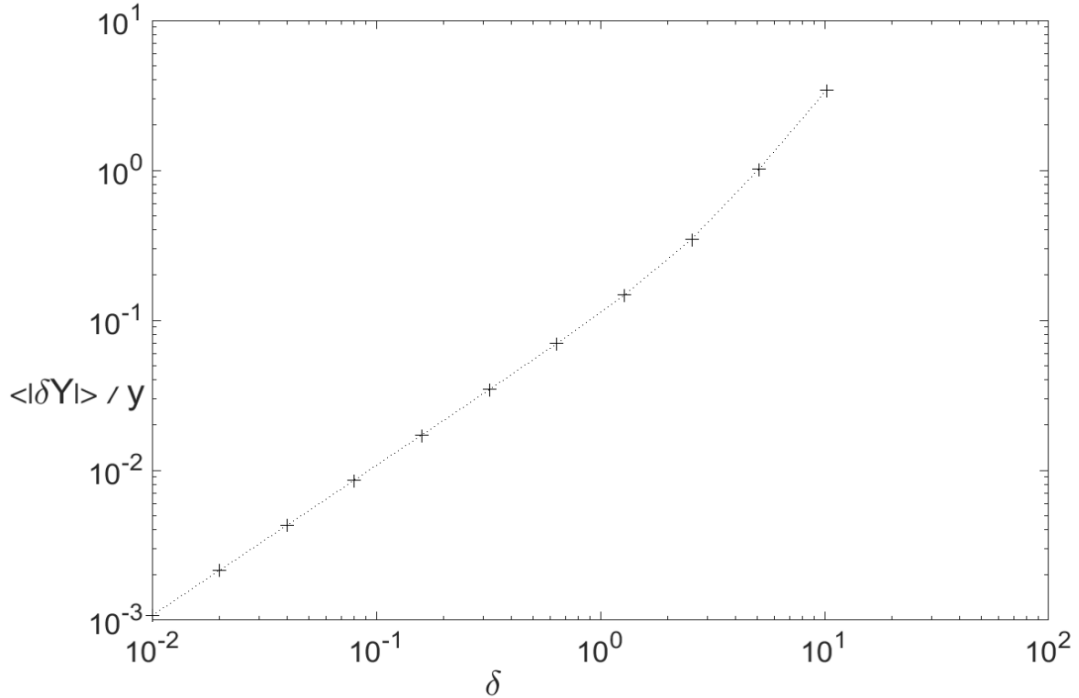


Fig. 12- The yield sensitivity $\langle |\delta Y| \rangle / Y$ for $N = 6, M = 4$.

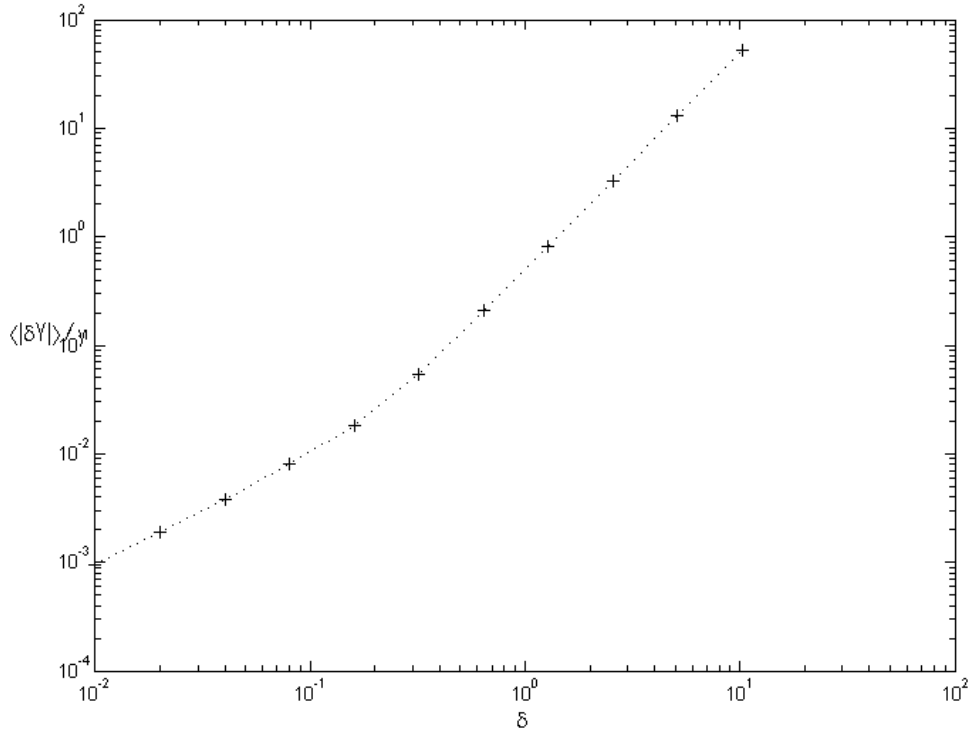


Fig. 13- The yield sensitivity $\langle |\delta Y| \rangle / Y$ for $N = 12, M = 8$.

Since small changes in δ result in large changes in the average of the deviation of the yield from its optimum (or equivalently to large deviations in the yield sensitivity) we may expect also the distribution of the yield to be very wide. The scale in the graphs describing those quantities suggest that if we would like to obtain a distribution, it would be reasonable to obtain the distribution of the logarithm of the yield rather than the distribution of the yield itself. Furthermore, after obtaining the distribution of δV and the distribution of the logarithm of the yield, it would be interesting to ask if somehow the deviation from the constraints is related to the deviation in the yield. It is natural to assume that the interpolation constraint reduces the yield considerably. Therefore we may expect that the larger δV is the larger is the yield. To check our first hypothesis we present first the distribution of the logarithm of the yield (Fig. 14). To check our second hypothesis, we present in Fig. 15 the scatter-plot of δV and δY for a fixed δ . Namely, we chose a thousand sets $\{\delta_m\}$ from the Gaussian distribution with standard deviation δ . For each set we obtain δV and δY and present the pair as a point in the $\delta V - \delta Y$ plane. Both graphs (Figs. 11 and 12) are presented for $\delta = 0.01$, $N = 12$ and $M = 8$.

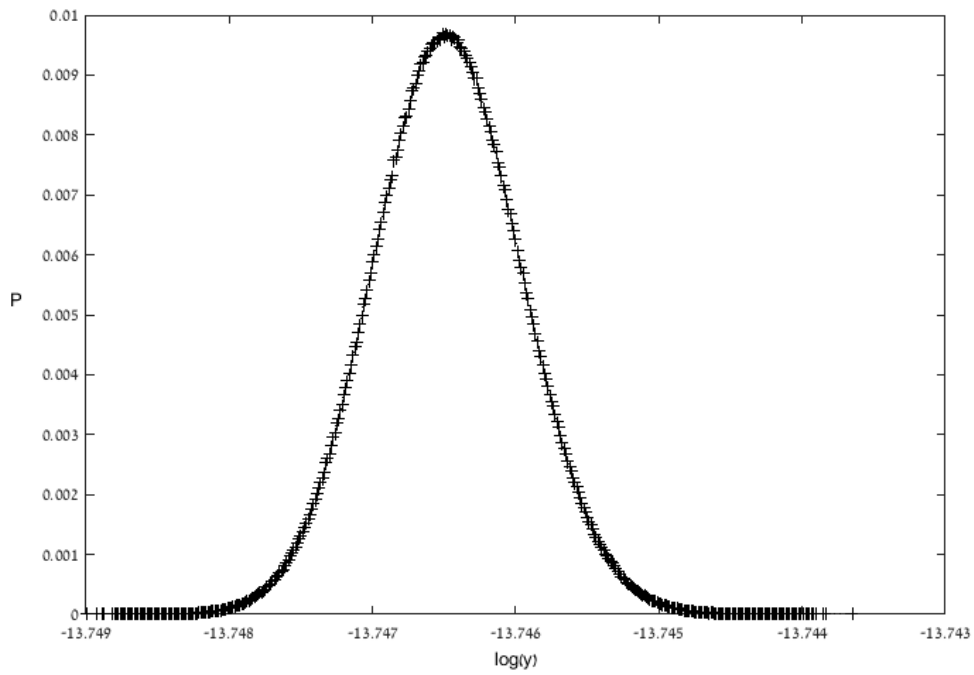


Fig. 14- The normalized distribution of the logarithm of the yield, for $\delta = 0.01$.

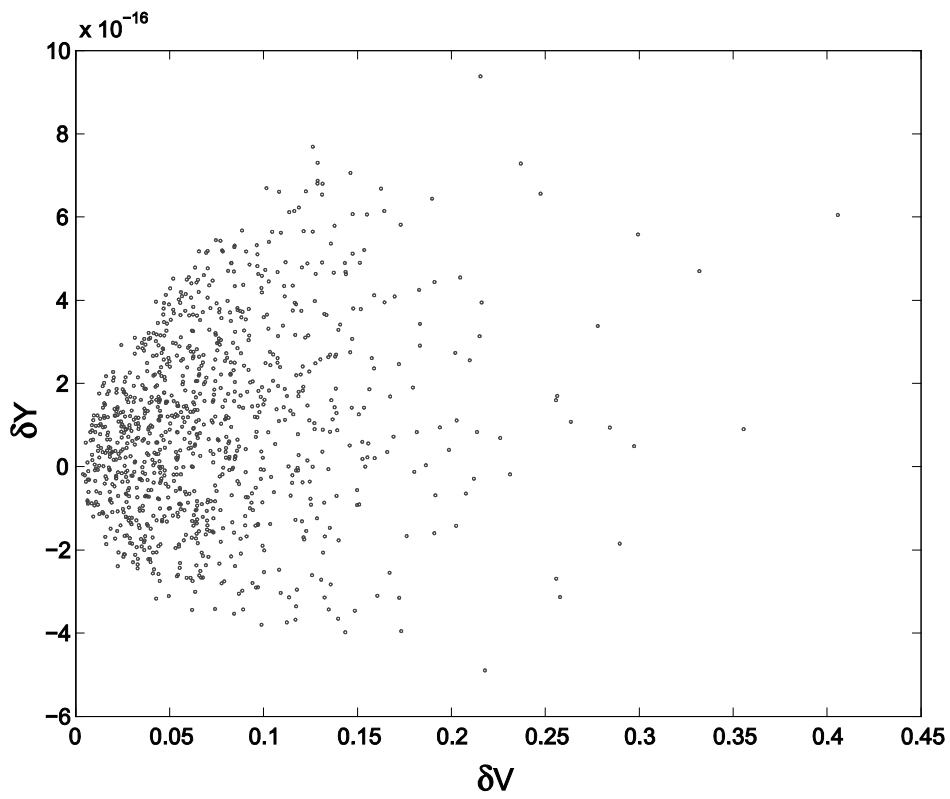


Fig. 15 - The scatter-plot of $(\delta V, \delta Y)$ for $\delta = 0.01$, $N = 12$ and $M = 8$.

We see first that indeed, the distribution of the logarithm of the yield is narrow and resembles a Gaussian. We also see that increasing δV tends to increase δY , with obvious tendency to have more positive δY 's than negative ones. Therefore, that the initial insight that relaxing the constraints will result in higher yields seems to be correct. This is actually the reason why the average $\langle \delta Y \rangle$ is always positive.

So far, we have characterized the departure from strict interpolation by the single parameter δV . It can occur, however, that while the departure from strict interpolation, as expressed by δV , is not that small, the signal still superoscillates with the prescribed number of oscillation in the appropriate interval. The opposite is also possible. Namely, although δV is relatively small, some oscillations may still be lost in the appropriate interval. With that in mind, we count the number of oscillations in the interval $(-a, a)$, and denote the number of missing oscillations in this superoscillation interval by Δn (in all the examples we used $a=1$). In Fig. 16 we present the average of Δn as a function of δ for the case $N=15, M=10$. As expected, the average depart from zero slowly, and stays fairly small even for δ 's that are not extremely small.

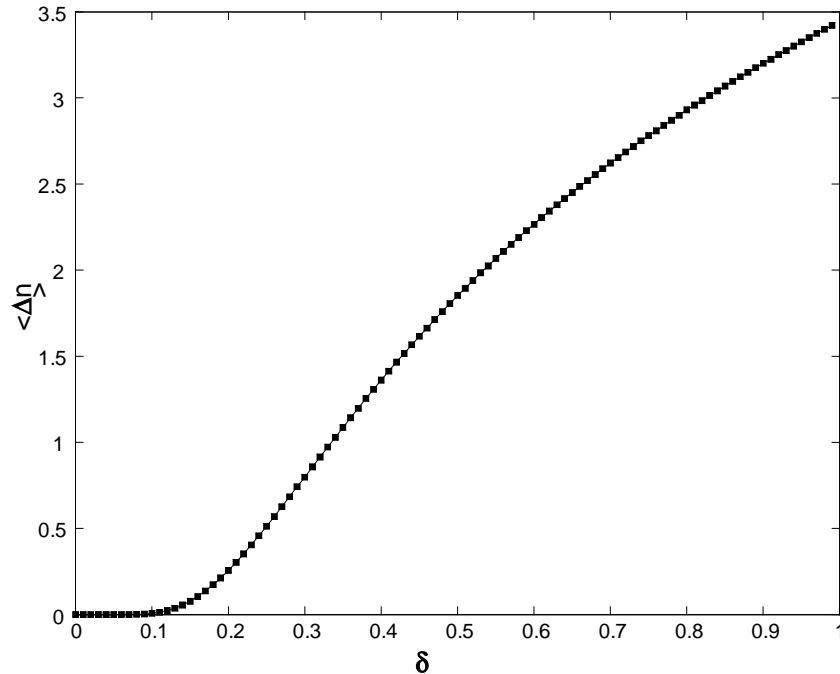


Fig. 16 -The average number of missing oscillations $\langle \Delta n \rangle$ as a function of of the error level δ for $N=15, M=10$.

The standard deviation of Δn as a function of δ is also a useful tool for assessing the loss of oscillations as a function of the error level δ , and we therefore present it below in Fig. 17.

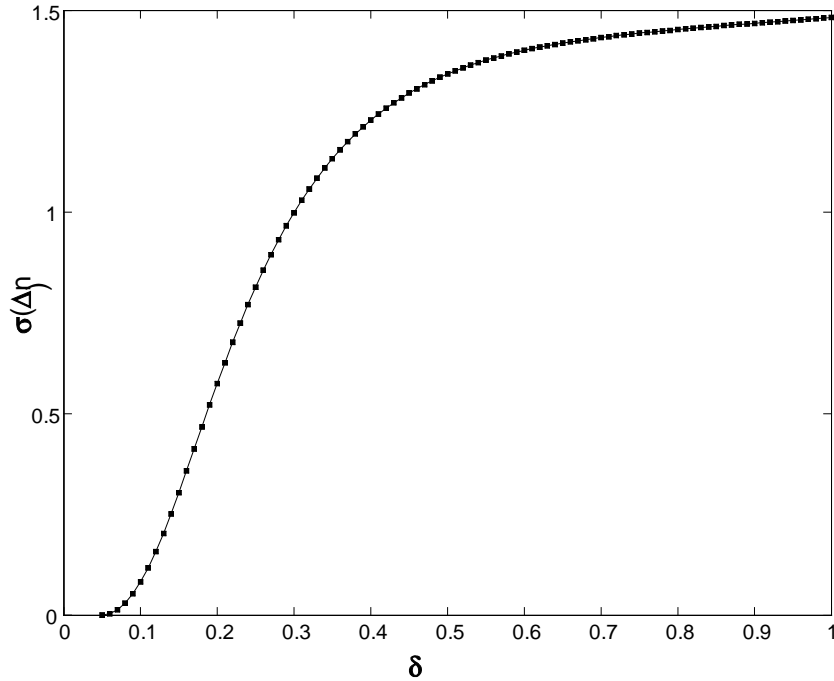


Fig. 17 - The standard deviation of the number of missing oscillations, as a function of δ for $N = 15, M = 10$.

To conclude, we have considered the effect of errors in the Fourier coefficients defining the signal, on the superoscillating yield and signal quality of interpolated superoscillations. Such an effect is abundant in any physical system that may use superoscillations and therefore analyzing it is of high importance both theoretically and from the point of view of applications.

We considered in detail two scenarios. In the first scenario, we analyzed deviations within the sub-space of exactly interpolating signals from that signal that minimizes the signal energy per period. We have also shown that that signal is very close to the signal of optimal yield within this sub-space. The second scenario is where errors in the Fourier coefficients of the low frequency components can violate the interpolation condition and thus can reduce the signal quality in the superoscillation portion. Such errors affect also the yield. To quantify these effects we define the Interpolation-sensitivity δV and Yield-sensitivity δY . Estimates on both sensitivities as a function of the number of the Fourier components and the standard deviation describing the uncorrelated errors in each of the Fourier coefficients have been obtained. We have also counted the number of missing oscillations Δn due to those errors. It is found that an error level δ in the Fourier components $\{A_m\}$ which is not too small still ensures superoscillation and can result in a yield which is larger

than the optimal one under the interpolation constraint. Namely, a slight relaxation of the strict constraint may still keep the required number of superoscillations yet result in an increased yield which can be a real advantage in application.

An important bottom line is that although generating optimized superoscillations may be a challenging task, once attained it is no longer very sensitive to error or noise, and can thus be realized in physical systems where this is abundant. Another important conclusion is that compromising the shape of the function in the superoscillatory region (such as the regularity of the oscillations and the location of their maxima/minima) can result in an improved superoscillatory yield, which could be advantageous.

Bibliography

[1] Y. Aharonov, D. Albert and L. Vaidman, "How the result of a measurement of a component of the spin of a spin- $1/2$ particle can turn out to be 100", *Phys. Rev. Lett.* Vol. **60**, no. 14, pp. 1351–1354, 1988.

[2] Y. Aharonov, S. Popescu and D. Rohrlich, "How can an infra-red photon behave as a gamma ray?" Tel-Aviv University *Preprint* TAUP 1847–90, 1990.

[3] M. V. Berry, "Evanescent and real waves in quantum billiards and Gaussian beams," *J. Phys. A: Math. Gen.*, vol. **27**, no. 11, pp.L391–L398, 1994.

[4] M. V. Berry, "Faster than Fourier in Quantum Coherence and Reality" *Celebration of The 60th Birthday of Yakir Aharonov* ed. J. S. Anandan and J. L. Safko (Singapore: World Scientific) pp 55–65, 1994.

[5] A. Kempf, "Black holes, bandwidths and Beethoven", *J. Math. Phys.*, Vol. **41**, no. 4, pp. 2360–2374, Apr. 2000.

[6] M. V. Berry and S. Popescu, "Evolution of quantum superoscillations and optical superresolution without evanescent waves", *J. Phys. A: Math. Gen.*, Vol. **39**, pp. 6965–6977, 2006.

[7] D. Slepian and H. O. Pollak, "Prolate spheroidal wave functions, Fourier analysis and uncertainty—I", *Bell Syst. Tech. J.*, Vol. **40**, no. 1, pp. 43–63, Jan. 1961.

[8] L. Levi, "Fitting a bandlimited signal to given points", *IEEE Trans. Inf.Theory*, Vol. **IT-11**, pp. 372–376, Jul. 1965.

- [9] D. Slepian, "Prolate spheroidal wave functions, Fourier analysis and uncertainty — V: The discrete case", *Bell Syst. Tech. J.*, Vol. **57**, no. 5, pp. 1371–1430, May 1978.
- [10] P. J. S. G. Ferreira and A. Kempf, "The energy expense of superoscillations", in *Signal Process. XI - Theories Applicat.: Proc. EUSIPCO-2002 XI Eur. Signal Process. Conf.*, Toulouse France, vol.II, pp. 347–350, Sep. 2002.
- [11] P. J. S. G. Ferreira and A. Kempf, "Superoscillations: Faster Than the Nyquist", *IEEE Trans. on Signal Processing*, Vol. **54**, no. 10, pp. 3732-3740, October 2006.
- [12] D. G. Lee and P. J. S. G. Ferreira, "Direct Construction of Superoscillations", *IEEE Trans. on Signal Processing*, vol. **62**, pp. 3125-3134, June 2014.
- [13] D. G. Lee and P. J. S. G. Ferreira, "Superoscillations of Prescribed Amplitude and Derivative", *IEEE Trans. on Signal Processing*, vol. **62**, pp. 3371-3378, July 2014.
- [14] N. I. Zheludov, "What diffraction limit?", *Nature Materials* vol. **7**, pp. 420-422, June 2008.
- [15] F. M. Huang and N. I. Zheludov, "Super-Resolution without Evanescent Waves", *Nano Letters*, vol. **9**, no 3 , pp. 1249-1254, 2009.
- [16] Z. Zalevsky, "Super-Resolved Imaging: Geometrical and Diffraction Approaches", Springer Verlag, Springer Briefs in Physics 2011.
- [17] G. Yuan et al., "Planar super-oscillatory lens for sub-diffraction optical needles at violet wavelengths", *Sci. Rep.* **4**, 6333 (2014).
- [18] E. T. F. Rogers et al., "A super-oscillatory lens optical microscope for subwavelength imaging", *Nature Materials* vol **11**, pp. 432-435 (2012).
- [19] J. Lindberg, "Mathematical concepts of optical superresolution", *J. Opt.*, Vol. **14**, 083001, 2012.
- [20] M. V. Berry and N. Moiseyev, " Superoscillations and supershifts in phase space: Wigner and Husimi function interpretations", *J. Phys. A: Math. And Theo.*, Vol. **47**, 315203, August 2014.
- [21] D. G. Baranov, A. P. Vinogradov and A. A. Lisyansky, "Abrupt Rabi oscillations in a superoscillating electric field", *Optics Letters*, Vol. **39**, pp. 6316-6319, November 2014.

- [22] Y. Eliezer and A. Bahabad, "Super-transmission:the delivery of superoscillations through the absorbing resonance of a dielectric medium", *Optics Express*, Vol. **22**, No. 25, December 2014.
- [23] D. G. Baranov, A. P. Vinogradov and A. A. Lisyansky, "Superoscillating response of a nonlinear system on a harmonic signal", arXiv:1505.04703.
- [24] R. Remez and A. Arie, "Super-narrow frequency conversion", *Optica*, vol. **2**, no. 5, May 2015.
- [25] D. G. Lee and P. J. S. G. Ferreira, "Superoscillations with Optimal Numerical Stability", *IEEE Signal Processing Letters*, vol. **21**, pp. 1443-1447, December 2014.
- [26] E. Katzav and M. Schwartz, "Yield Optimized Superoscillations", *IEEE Trans. on Signal Proc.* Vol. **61**,no 12, pp 3113-3118, 2013.
- [27] D. G. Lee and P. J. S. G. Ferreira, "Superoscillations With Optimum Energy Concentration", *IEEE Trans. on Signal Processing*, vol. **62**, pp. 4857-4867, September 2014.
- [28] F. W. J. Olver, D. W. Lozier, R. F. Boisvert, and C. W. Clark, editors. *NIST Handbook of Mathematical Functions*. Cambridge University Press, New York, NY, 2010.